Proceedings of the ASME 2009 International Design Engineering Technical Conferences & Computers and Information in Engineering Conference
IDETC/CIE 2009
August 30-September 2, 2009, San Diego, USA

DETC2009-87620

VIBRATION ISOLATION VIA LINEAR AND NONLINEAR PERIODIC DEVICES

A. Spadoni

GALCIT
California Institute of Technology
Pasadena CA, 91125
Email: spadoni@caltech.edu

C. Daraio*

GALCIT
California Institute of Technology
Pasadena CA, 91125
Email: daraio@caltech.edu

ABSTRACT

The current manuscripts deals with the design of passive mechanical filters for vibration attenuation a low frequencies. Traditionally, this has been addressed employing dissipation as the attenuation mechanism. While such strategy provides broad-frequency effectiveness, attenuation at any given frequency is modest. Mass and stiffness-modulated periodic systems, on the other hand, exploit dispersion as the attenuation mechanism and represent an alternative to dissipation-based devices. Attenuation due to dispersion may be significantly higher than what is afforded by dissipation-based systems within a design frequency rage. The proposed assemblies, however, are not easily tailored to filter lowe-frequency vibrations. To this end, embedding such periodic systems into an elastic matrix yields a high-pass mechanical filter with tunable stop bands were waves are not allowed to propagate. Significant improvements in performance moreover may be obtained if intrinsically nonlinear devices are adopted. Specifically, a strongly nonlinear medium such as ordered granular media supports a limited number of waveforms, resulting in an efficient mechanical filter. Results reported here, in fact, suggest matrix-embedded sphere chains as highly tunable mechanical filters for vibration attenuation.

1 Introduction

Vibration isolation or even partial reduction is a daunting endeavor that has been at the forefront of research efforts by the structural dynamics community. The myriad proposed or employed solutions fall under two broad categories: passive and active systems. In the former case, the intrinsic material and geometric properties of a device are exploited to reduce vibrations over certain frequency bands. Passive systems exploiting dissipative or viscoelastic characteristics of a material, for example, are designed to be effective over broad frequency bands, but may not provide significant damping. Other passive systems, such as tunable mass dampers are very effective in reducing vibrations, but only over very narrow frequency bands. In order to alleviate such shortcomings, tunable active systems have been designed to be effective over significant frequency bands and at the same time provide significant attenuation [1]. In the latter case, however, the infrastructure necessary to achieve broadband and significant damping may offset any benefits.

In recent years, a number of passive designs have been introduced which, at least theoretically, can annihilate vibrations over multiple frequency regions (band gaps). Such systems exploit periodicity to reduce vibrations via dispersive phenomena instead of dissipative mechanisms [1–5]. More recent investigations seek to enhance the already promising periodic systems by introducing nonlinearity, which may provide significant tunability [6–9]. In this work, the benefits of periodic devices, both linear and nonlinear, for low-frequency vibration suppression will addressed. Namely, a number of assemblies, including chains of granular media, will be studied both numerically and analytically with the aim of demonstrating the advantages of introducing nonlinearity.

*Address all correspondence to this author.

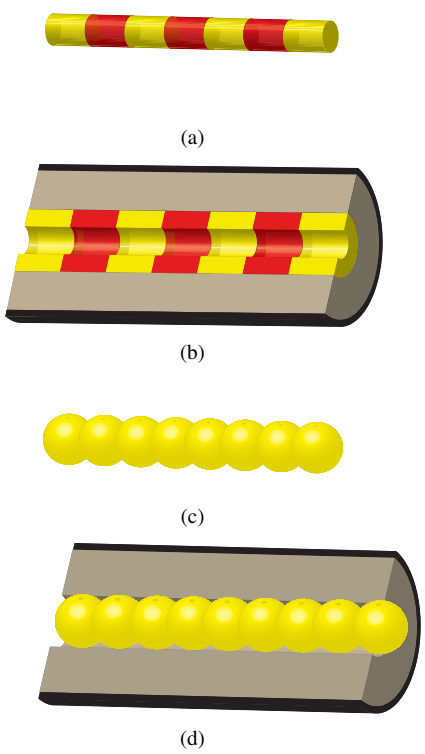

Figure 1. Considered mechanical filters: (a) bi-material rod, (b) bi-material rod embedded in a matrix, (c) chain of spheres, and (d) chain of spheres embedded in a matrix

2 Theory

Vibration attenuation is commonly achieved by exploiting dissipative effects [10]. Similar results can be obtained by exploiting dispersive effects characteristic of periodic systems exhibiting both pass and stop bands [11, 12], whereby wave propagation is allowed or forbidden respectively. While theoretically both strategies may appear as effective, dispersion produced by periodic systems is still to be adopted as a practical means for vibration reduction, even though a number of possible implementations have been proposed [13, 14]. Recent studies aimed at quantifying the effects of nonlinear characteristics in the design of vibration-absorbing systems have uncovered periodic as well as non-periodic assemblies whose dispersion relation is amplitude dependent [7, 15]. The objective of the current work is to study improved linear devices for vibration absorption as well as to quantify potential benefits derived from including nonlinear characteristics in the proposed systems.

2.1 Linear filters

The simplest example of a periodic assembly producing dispersion in dynamic signals may be represented by a bi-material rod, like the one depicted in fig. 1.a. This is a practical implementation of the idealized and ubiquitous model of alternating masses and springs. In a chain of masses and springs, periodic modulation of mass produces stop bands or band gaps [16]; in such simple example, periodic modulation of spring stiffness alone on the other hand, does not produce any band gaps. For a

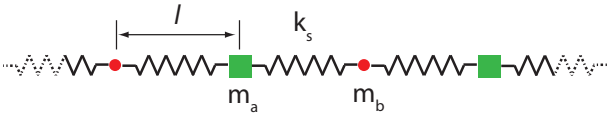

Figure 2. Simplest periodic system: spring-mass chain

spring-mass chain like the one depicted in fig. 2, the dispersion relation is [16]:

$$\omega_{\pm} = k_s \left(\frac{1}{m_a} + \frac{1}{m_b} \right) \pm \sqrt{k_s^2 \left(\frac{1}{m_a} + \frac{1}{m_b} \right)^2 - \frac{4k_s^2}{m_a m_b} \sin^2 \mu l} \quad (1)$$

where m_a, m_b, denote the mass of point a and b respectively, k_s the spring stiffness, while μ and l are the wavenumber and distance between masses. Additionally, ω_+ and ω_- are termed the optical and acoustic branch of the dispersion relation respectively. The optical branch has a minimum at $\omega_+ = \sqrt{2k_s/m_b}$ while the acoustic branch has a maximum at $\omega_- = \sqrt{2k_s/m_a}$. A region of forbidden wave propagation is thus obtained if $m_a > m_b$. Within this frequency region, the wavenumber becomes a complex number whose imaginary part indicates the phase of propagation while its real part denotes attenuation. Any mechanical disturbance characterized by forbidden frequencies will attenuate; if this system is infinite such signal will not reach the opposite end of the chain, and its amplitude will decay exponentially to 0. In practical situations however, any device will be far from ideal, and the amplitude of attenuation is to be considered. A system of very limited extent for example may yield very little vibration reduction even if the attenuation constant were to be large. An additional challenge is posed by the need to attenuate signals at low frequencies in addition to providing load-bearing capabilities. From eq. (1), low-frequency band gaps require that the acoustic-branch maximum $\omega_- = \sqrt{2k_s/m_a}$ be small, yielding a system with either low stiffness or high mass. Such characteristics are seldom desirable.

Vibration reduction, especially at low frequencies, may be enhanced if any mechanical filter is embedded in an elastic matrix. To this end, it is useful to analyze the dispersion relation of a generalized rod, which includes both restoring forces associated with the surrounding matrix and intrinsic dissipative effects. The

motion of such one-dimensional medium, illustrated in fig. 1.b, in absence of external loads can be expressed as:

$$\frac{\partial}{\partial x}\left(EA\frac{\partial u}{\partial x}\right)-\rho A\frac{\partial^2 u}{\partial t^2}-\rho_f A_f\frac{\partial^2 u}{\partial t^2}-\eta\frac{\partial u}{\partial t}-K_f u=0, \qquad (2)$$

where $u=u(x,t)$ indicates displacement, E the Young's modulus, A the rod's cross-sectional area, ρ the density, and η denotes the damping coefficient of the rod's material. The surrounding matrix has a density ρ_f, an equivalent stiffness K_f (with units of N/m^2) and contacts the rod over the surface A_f. The elastic and dynamic contribution of the surrounding matrix is here included in the equation of motion (eq. (2)) as a Winkler foundation model [17]. The resulting dispersion relation upon assuming harmonic motion in time and constant cross-sectional area is [18]:

$$\mu=\pm\sqrt{\frac{\rho A+\rho_f A_f}{EA_f}\omega^2-i\frac{\eta}{EA}-\frac{K_f}{EA}}, \qquad (3)$$

where $i=\sqrt{-1}$ and μ indicates the wavenumber as before. Neglecting damping effects, which are usually small, one obtains a cut-off frequency ω_c below which wave propagation is attenuated, or the wavenumber becomes a complex number

$$\omega_c^2=\frac{K_f}{\rho A+\rho_f A_f}. \qquad (4)$$

Embedding a bi-material rod into an elastic matrix hence provides the opportunity to design a high-pass filter with additional attenuation controlled by periodic stiffness and mass modulation. The combination of a bi-material rod embedded into an elastic medium is addressed numerically in the following section.

2.2 Linear models: rods and matrix-embedded rods

The total energy in a mechanical system may be expressed as:

$$\Pi=U+V+K-W \qquad (5)$$

where U is the strain energy, V is the potential energy, K the kinetic energy, and W is the work done by externally applied loads. More specifically, introducing stress σ, strain ε and displacement u variables, eq. (5) can be recast as:

$$\Pi=\frac{1}{2}\int_V \boldsymbol{\varepsilon}^T\boldsymbol{\sigma}\,dV+\frac{1}{2}\int_A \phi\,dA+\frac{1}{2}\int_V \rho\dot{\boldsymbol{u}}^T\dot{\boldsymbol{u}}\,dV-W, \qquad (6)$$

where, ϕ is a potential introduced to account for external influences and will be determined by the specific problem at hand. Since only the elastically 1D models shown in fig. 3 will be

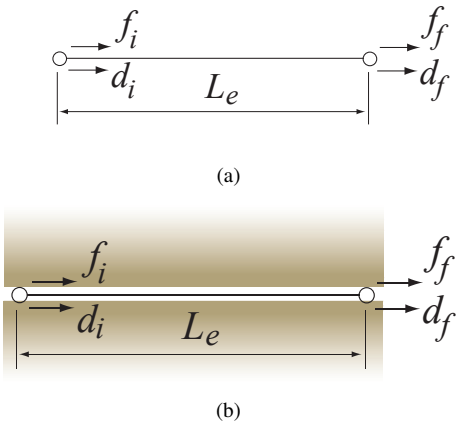

Figure 3. 1D bar element (a), 1D bar element embedded in a matrix (b)

treated, the mechanical stress, strain and displacement vectors are defined respectively as: $\boldsymbol{\sigma}=\{\sigma_x\}^T$, $\boldsymbol{\varepsilon}=\{\varepsilon_x\}^T$, and $\boldsymbol{u}=\{u\}^T$. The models considered here are discretized via finite elements, in particular:

$$\begin{aligned} u&=\boldsymbol{N}\boldsymbol{d}^e\\ \varepsilon&=\boldsymbol{B}\boldsymbol{d}^e\\ \sigma&=E\varepsilon \end{aligned} \qquad (7)$$

where $\boldsymbol{d}^e=\{d_i\ d_f\}^T$ is the element nodal degree-of-freedom (DOF) vector, $\boldsymbol{N}=\{1-x/L_e\ \ x/L_e\}$ is the vector of interpolating or shape functions, and $\boldsymbol{B}=[\partial]\boldsymbol{N}$ is the strain interpolation matrix. The element length is denoted by L_e and the Young's modulus by E. Substituting eq. (7) into eq. (6) and imposing equilibrium by enforcing that the total potential be at a minimum:

$$\delta\Pi=0, \qquad (8)$$

leads to the following governing equations in matrix form

$$\boldsymbol{M}\ddot{\boldsymbol{d}}+\boldsymbol{K}\boldsymbol{d}=\boldsymbol{f}, \qquad (9)$$

where $\boldsymbol{M}$ and $\boldsymbol{K}$ are the mass and stiffness matrices, while $\boldsymbol{d}$ and $\boldsymbol{f}$ are the global nodal displacement and load vectors respectively.

In the case of the bi-material bar, shown in fig. 1.a, the potential ϕ in eq. (6) is absent as no external phenomena are considered. Accordingly, the stiffness and mass matrices are:

$$\boldsymbol{K} = \int_V \boldsymbol{B}^T E \boldsymbol{B} dV \tag{10}$$

$$\boldsymbol{M} = \int_V \rho \boldsymbol{N}^T \boldsymbol{N} dV \tag{11}$$

For the case where the bi-material rod is surrounded by a matrix, as depicted in fig. 1.b, the matrix itself is included in the equations as a Winkler foundation model [17] and the associated potential is $\phi = \frac{1}{2}\beta u^2$. Here, β is the foundation modulus with units of pressure per unit length. The stiffness matrix must now be augmented with the effects of the surrounding matrix as follows [17]:

$$\boldsymbol{K} = \int_V \boldsymbol{B}^T E \boldsymbol{B}\, dV + \int_{\partial V} \beta \boldsymbol{N}^T \boldsymbol{N}\, d\partial V, \tag{12}$$

where ∂V is the area in contact with the rod in consideration. Inertial effects of the surrounding medium are here neglected and thus the mass matrix is identical to that of eq. (11).

2.2.1 Wave propagation analysis Given the periodicity for either the bi-material rod or the same rod embedded in a matrix, illustrated in figs. 1.a and 1.b respectively, their performance and mechanical filters may be quantified by analyzing a single unit cell, such as the one depicted in fig. 4, and assuming that the underlying motion be harmonic. In fig. 4, the subscripts

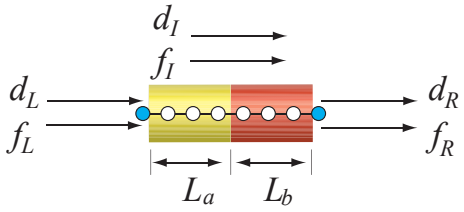

Figure 4. FE discretization of a unit cell

$()_L$, $()_R$, and $()_I$ denote quantities belonging to the left side of the unit cell, the right side and the internal values respectively.

The transfer matrix technique is here employed to obtain the dispersion relations of each of the considered linear models. In the procedure described in what follows, the unknown quantity is the wavenumber μ while the frequency ω is known. Assuming harmonic motion and having ω as an input parameter, eq. (9) can be recast as

$$\left[\boldsymbol{K} - \omega^2 \boldsymbol{M}\right] \boldsymbol{d} = \boldsymbol{K}_D(\omega)\, \boldsymbol{d} = \boldsymbol{f}, \tag{13}$$

where $\boldsymbol{K}_D$ denotes the dynamic stiffness matrix. Nodal DOF's and nodal loads can be organized as $\boldsymbol{d} = \{\boldsymbol{d}_L\, \boldsymbol{d}_I\, \boldsymbol{d}_R\}^T$ and $\boldsymbol{f} = \{\boldsymbol{f}_L\, \boldsymbol{f}_I\, \boldsymbol{f}_R\}^T$. Due to equilibrium considerations, the absence of externally applied forces and the considered periodicity conditions, $\boldsymbol{f}_I = \boldsymbol{0}$. Accordingly, eq. (13) can be rewritten as follows:

$$\boldsymbol{K}_D(\omega) \begin{Bmatrix} \boldsymbol{d}_L \\ \boldsymbol{d}_I \\ \boldsymbol{d}_R \end{Bmatrix} = \begin{bmatrix} \boldsymbol{\alpha}_{L,L} & \boldsymbol{\alpha}_{L,I} & \boldsymbol{\alpha}_{L,R} \\ \boldsymbol{\alpha}_{I,L} & \boldsymbol{\alpha}_{I,I} & \boldsymbol{\alpha}_{I,R} \\ \boldsymbol{\alpha}_{R,L} & \boldsymbol{\alpha}_{R,I} & \boldsymbol{\alpha}_{R,R} \end{bmatrix} \begin{Bmatrix} \boldsymbol{d}_L \\ \boldsymbol{d}_I \\ \boldsymbol{d}_R \end{Bmatrix} = \begin{Bmatrix} \boldsymbol{f}_L \\ \boldsymbol{0} \\ \boldsymbol{f}_R \end{Bmatrix} \tag{14}$$

Equation (14) can be re-cast into transfer matrix form through the condensation of the internal degrees of freedom and by imposing relations between left and right displacements and forces. This gives:

$$\begin{Bmatrix} \boldsymbol{d}_R \\ \boldsymbol{f}_R \end{Bmatrix} = \boldsymbol{T}(\omega) \begin{Bmatrix} \boldsymbol{d}_L \\ \boldsymbol{f}_L \end{Bmatrix} \tag{15}$$

where

$$\boldsymbol{T}(\omega) = \begin{Bmatrix} -\hat{\boldsymbol{\alpha}}_{L,R}^{-1}\hat{\boldsymbol{\alpha}}_{L,L} & \hat{\boldsymbol{\alpha}}_{L,R}^{-1} \\ \hat{\boldsymbol{\alpha}}_{R,R}(\hat{\boldsymbol{\alpha}}_{L,R}^{-1}\hat{\boldsymbol{\alpha}}_{L,L}) - \hat{\boldsymbol{\alpha}}_{R,L} & -\hat{\boldsymbol{\alpha}}_{R,R}^{-1}\hat{\boldsymbol{\alpha}}_{L,R} \end{Bmatrix} \tag{16}$$

with:

$$\begin{aligned} \hat{\boldsymbol{\alpha}}_{\mathcal{L},\mathcal{L}} &= \boldsymbol{\alpha}_{\mathcal{L},\mathcal{L}} - \boldsymbol{\alpha}_{\mathcal{L},I}\boldsymbol{\alpha}_{\mathcal{L},\mathcal{L}}^{-1}\boldsymbol{\alpha}_{I,\mathcal{L}}, \\ \hat{\boldsymbol{\alpha}}_{\mathcal{L},\mathcal{R}} &= \boldsymbol{\alpha}_{\mathcal{L},\mathcal{R}} - \boldsymbol{\alpha}_{\mathcal{L},I}(\boldsymbol{\alpha}_{I,I}^{-1}\boldsymbol{\alpha}_{I,\mathcal{R}}), \\ \hat{\boldsymbol{\alpha}}_{\mathcal{R},\mathcal{L}} &= \boldsymbol{\alpha}_{\mathcal{R},\mathcal{L}} - \boldsymbol{\alpha}_{\mathcal{R},I}(\boldsymbol{\alpha}_{I,I}^{-1}\boldsymbol{\alpha}_{I,\mathcal{L}}), \\ \hat{\boldsymbol{\alpha}}_{\mathcal{R},\mathcal{R}} &= \boldsymbol{\alpha}_{\mathcal{R},\mathcal{R}} - \boldsymbol{\alpha}_{\mathcal{R},I}(\boldsymbol{\alpha}_{\mathcal{L},\mathcal{L}}^{-1}\boldsymbol{\alpha}_{I,\mathcal{R}}) \end{aligned}$$

The eigenvalues of the transfer matrix $\boldsymbol{T}(\omega)$ can be obtained through the solution of the following eigenvalue problem:

$$\boldsymbol{T}(\omega) \begin{Bmatrix} \boldsymbol{d}_L \\ \boldsymbol{f}_L \end{Bmatrix} = \lambda(\omega) \begin{Bmatrix} \boldsymbol{d}_L \\ \boldsymbol{f}_L \end{Bmatrix} \tag{17}$$

Combining eq.s (15) and (17) gives:

$$\begin{Bmatrix} \boldsymbol{d}_R \\ \boldsymbol{f}_R \end{Bmatrix} = \lambda(\mu_y = 0, \omega) \begin{Bmatrix} \boldsymbol{d}_L \\ \boldsymbol{f}_L \end{Bmatrix} \tag{18}$$

which indicates that the state vectors at the left and right of the unit cell identified by the particular direction of wave propagation are related through the eigenvalues of the transfer matrix. The eigenvalues therefore determine the nature of the wave dynamics in the periodic structure. Waves are free to propagate in the specified direction for those values of frequency for which $|\lambda| = 1$, whereas attenuation occurs if $|\lambda| < 1$. The wavenumber μ, accordingly, can be an complex number or $\mu = \delta + i\varepsilon$, where δ is known as the attenuation constant and ε is the propagation constant. The wavenumber μ corresponding to the assigned value of frequency ω can be obtained by letting

$$\lambda = e^{\mu(L_a+L_b)} \tag{19}$$

which is an expression that yields both imaginary and real parts of the wavenumber μ.

2.3 Nonlinear filters

While the nonlinear chain of spring and masses proposed in [15] does feature tunable characteristics, chains of metal spheres promise more ample control over the nature of the signals allowed to propagate. For this reason, only the latter configuration will be investigated as a potential vibration-absorbing device.

Assuming that the propagating signals within a one dimensional chain of spheres are such that no plastic flow takes place (see [6] for necessary conditions), the interaction between any two spheres can be modeled via Hertz contact law [19]. In this manner, each sphere is model as a point mass and the interaction between such masses is governed by nonlinear springs as shown in fig. 5.a. In particular, the relationship between force F_{ij} and deformation δ_{ij} between neighboring spheres i and j is [19]

$$F_{ij} = k_{ij}\delta_{ij}^{3/2}, \tag{20}$$

where

$$k_{ij} = \frac{4E_iE_j}{3E_i\left(1-\nu_j^2\right)+3E_j\left(1-\nu_i^2\right)}\sqrt{\frac{R_iR_j}{R_i+R_j}}, \tag{21}$$

and

$$\delta_{ij} = \begin{cases} (R_i+R_j)-|x_i+x_j|, & (R_i+R_j)-|x_i+x_j| > 0 \\ 0, & (R_i+R_j)-|x_i+x_j| \leq 0 \end{cases}, \tag{22}$$

where the notation $|\ |$ indicates absolute value. The governing equation of motion for the i^{th} neighboring sphere $j-1$ to the left and sphere $j+1$ to the right is obtained from the free-body diagram of fig. 5.b as

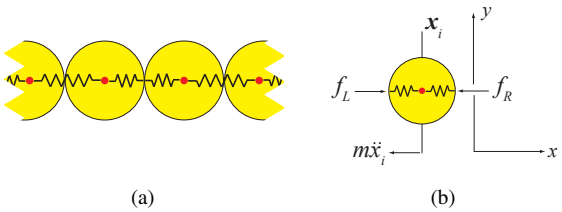

Figure 5. Idealized mechanical model for a sphere chain (a) with associated free-body diagram (b)

$$m_i\frac{d^2u_i}{dt^2} = F_{i,j-1} - F_{i,j+1}. \tag{23}$$

If the sphere chain is embedded in an elastic matrix with equivalent stiffness K_f as illustrated in fig. 1.d, the governing equation for the i^{th} sphere is

$$m_i\frac{d^2u_i}{dt^2} = F_{i,j-1} - F_{i,j+1} - K_fu_i. \tag{24}$$

Inertial effects stemming from the mass of the surrounding matrix are disregarded for simplicity and due to the fact that are expected to lower the cut-off frequency in a linear fashion as indicated by eq. (4). Both in the presence or absence of a surrounding matrix, the motion of each sphere in a one dimensional arrangement yields systems of nonlinear ordinary differential equations which can be integrated with the explicit Runge-Kutta scheme for example.

The nature of mechanical disturbances propagating within chains of spheres is unique in that the phase velocity strongly depends upon the initial strain state of the system, and there exist no speed of sound [6]. In the absence of initial strain, the propagating signals are solitons of fixed width ($10 \times R$) whose velocity depends on material properties, input amplitude and sphere radius R. In the following section, the performance of both linear, linear embedded as well as nonlinear systems are discussed. Insofar as nonlinear systems, no initial strain is considered as its effects are still being quantified.

3 Results and discussion

The dispersion relation for one dimensional signals propagating through a linear rod is linear and can be obtained from eq. (3). For a uniform rod not surrounded by any medium $\omega = \pm\sqrt{E/\rho}\,\mu$. This is depicted in fig. 6.a, where the wavenum-

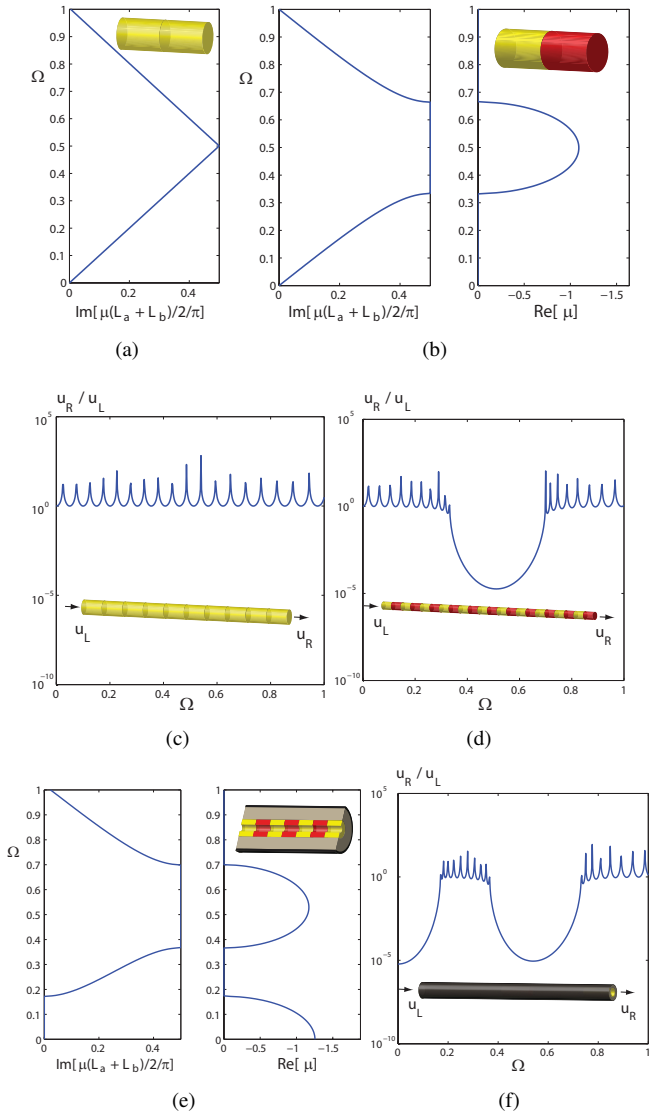

Figure 6. Dispersion relations form a uniform rod (a), bi-material rod (b) with associated FRF's shown in sub figures (c) and (d) respectively. Dispersion relation for a bi-material rod embedded in an elastic matrix (e) with associated FRF (f). All periodic configurations are composed of 10 unit cells

ber μ is always an imaginary number indicating no attenuation due to mass or stiffness modulation. The frequency considered in all the following cases is the normalized frequency $\Omega = \omega/(2\pi\sqrt{E_1/rho_1}/L)$, where L is the total length of the unit cell and E_1 and ρ_1 denote the Young's modulus and density associated with the acoustic branch of the dispersion relation. A free bi-material rod with $E_2/E_1 = 3$ and $\rho_2/\rho_1 = 3$, such as the case of aluminum and steel is characterized by the dispersion relation shown in fig. 6.b. In this case a band gap is present and the real part of the wavenumer μ denotes the extent of attenuation of waves traveling from one cell to the next. The frequency-response function FRF for both a uniform and bi-material rods (the latter composed of 10 unit cells) is shown in figs. 6.c and 6.d, where in the case of the latter configuration, vibrations characterized by frequencies within the band gap are significantly attenuated. Embedding a bi-material rod in an elastic matrix produces the dispersion relation illustrated in fig. 6.e, where a high-pass filter behavior is observed. For the case at hand, the equivalent foundation stiffness K_f is chosen as $K_f = 30E_2$ to clearly demonstrate its effect on both pass and stop bands. In particular, the cut-off frequency ω_c and extent of attenuation are linearly proportional to the value of K_f. The higher the cut-off frequency and/or desired attenuation, the higher is the value of K_f. The FRF for an embedded bi-material rod (fig. 6.f) confirms the high-pass behavior observed in the associated dispersion relation.

The results reported below are those for a chain composed of 31 steel spheres with Young's modulus $E = 210$ GPa, density $\rho = 8100$ Kg/m^3 and radius $R = 4.8$ mm. The system is impacted by a steel sphere with identical material and geometric properties as those of the chain and traveling with initial velocity of 0.5 m/s. The stiffness constant governing the contact interaction reported in eq. (21) is $k_i = 7.15 \times 10^9$ N/m. In absence of a surrounding medium, the chain of spheres depicted in fig. 1.c already provides filtering capabilities, as only two harmonics are expected to be transmitted, owing to the form of propagating signals [6]. This is shown in figs. 7.a and 7.b where the Morlet wavelet transforms of the velocity of mass 2 and 28 indicate how the frequency content evolves in time. For the same of completeness, the contact forces between spheres 2-3 and spheres 28-29 are superimposed. In the case where the chain of steel spheres is embedded in a soft matrix, with $K_f = 1$ KN/m for example, no effect is observed on the traveling disturbances, as shown in figs. 7.c and 7.d. If the the stiffness of the surrounding medium is increased to $K_f = 1$ MN/m on the other hand, signals with frequency content below 3 KHz are significantly attenuated (figs. 7.e and 7.f). Most interestingly, if the matrix stiffness is increased to $K_f = 100$ MN/m, now comparable with the stiffness governing the contact interaction between any two spheres, any signals with frequency content below 22 KHz are forbidden, or significantly attenuated as illustrated in figs. 7.g and 7.h.

4 Conclusions

The current manuscript proposes the adoption of stiffness and/or mass-modulated systems for vibration reduction via wave dispersion. While such devices offer a potential alternative to systems that exploit dissipation as the vibration-reduction mechanism, the attenuation of low-frequency signals, in particular, presents a challenge difficult to meet by simply modulating mass and stiffness. To this end, results reported in the current work seek to exploit the fact that embedding a dynamic system within

an elastic medium yields a mechanical high-pass filter. The performance of periodic systems for vibration absorption can thus be enhanced to address low-frequency signal attenuation. Nonlinear systems moreover are proposed as tunable devices capable of delivering similar performance as their linear counterparts. Specifically, a chain of steel spheres is shown to intrinsically act as a band pass filter whose center frequency varies with signal amplitude. Whenever such highly nonlinear medium is embedded in an elastic matrix, significant filtering capabilities may be obtained.

ACKNOWLEDGMENT

This work was developed in partnership with the aerospace research labs at Northrop Grumman Aerospace Systems. We thank Michal Brown for support of this research.

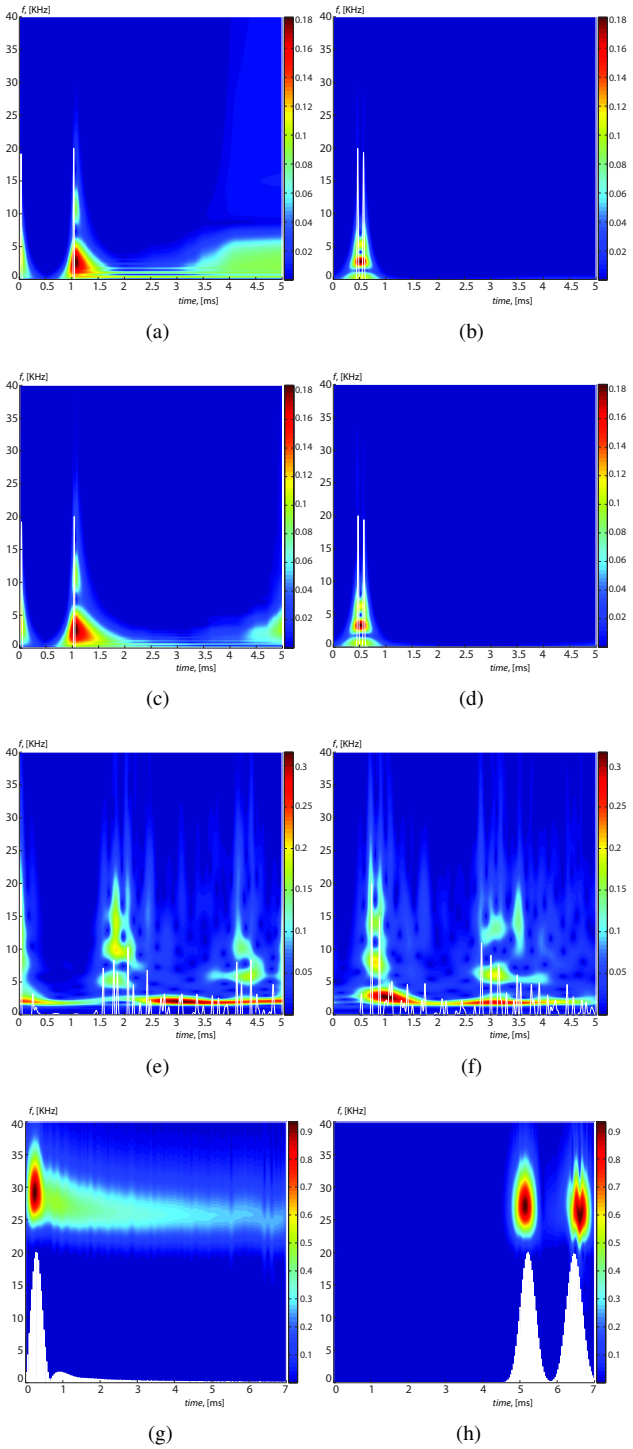

Figure 7. wavelet transform of velocity of mass 2 (a) and 28 (b) for $K_f = 0$ Pa; wavelet transform of velocity of mass 2 (c) and 28 (d) for $K_f = 1$ KN/m; wavelet transform of velocity of mass 2 (e) and 28 (f) for $K_f = 1$ MN/m; wavelet transform of velocity of mass 2 (g) and 28 (h) for $K_f = 100$ MN/m

REFERENCES

[1] Andre Preumont. *Vibration control of active structures*. Kluwer Academic Publishers, 2^{nd} edition, 2001.

[2] A. Spadoni and M. Ruzzene. Structural and acoustic behavior of chiral truss-core beams. *Journal of Vibration and Acoustics*, 128:616, 2006.

[3] A. Spadoni, M. Ruzzene, and K. A. Cunefare. Vibration and wave propagation control of plates with periodic arrays of shunted piezoelectric patches. *ournal of Intelligent Materials Systems and Structures*, in press, 2009.

[4] A. S. Phani, J. Woodhouse, and N. A. Fleck. Wave propagation in two-dimensional periodic lattices. *Journal of the Acoustical Society of America*, 119(4):1995 – 2005, 2006.

[5] M. El-Raheb and P. Wagner. Transmission of sound across a trusslike periodic panel; 2-d analysis. *Journal of the Acoustical Society of America*, 102(4):2176 – 2183, 1997.

[6] V. F. Nesterenko. *Dynamics of heterogeneous materials*. Springer-Verlag, New York, NY, 2001.

[7] E.B. Herbold, J. Kim, V. F. Nesterenko, S. Wang, and C Daraio. Tunable frequency band-gap and pulse propagation in a strongly nonlinear diatomic chain. *Acta Mechanica*, 205:85103, 2009.

[8] C. Coste and B. Gilles. On the validity of Hertz contact law for granular material acoustics. *The European Physical Journal B-Condensed Matter and Complex Systems*, 7(1):155–168, 1999.

[9] C. Daraio, V. F. Nesterenko, E. B. Herbold, , and S. Jin. Tunability of solitary wave properties in one-dimensional strongly nonlinear phononic crystals. *Physical Review E*, 73:026610, 2006.

[10] Andre Preumont. *Mechatronics: Dynamics of Electromechanical and Piezoelectric Systems*. Springer, 2006.

[11] D. J. Mead. A general theory of harmonic wave propagation in linear periodic systems with multiple coupling. *Journal of Sound and Vibration*, 27(2):235–260, 1973.

[12] D. J. Mead. Wave propagation in continuous periodic structures: research contribution from south hampton, 1964-1995. *Journal of Sound and Vibration*, 190(3):495–524, 1996.

[13] M. Ruzzene. Vibration and sound radiation of sandwich beams with honeycombs. *Journal of Sound and Vibration*, 277:741–763, 2004.

[14] O. Thorp, M. Ruzzene, and A. Baz. Attenuation of wave propagation in fluid-loaded shells with periodic shunted piezoelectric rings. *Smart Materials and Structures*, 10:893 – 906, 2001.

[15] B. S. Lazarov and J. S. Jensen. Low-frequency band gaps in chains with attached non-linear oscillators. *International Journal of Non-linear Mechanics*, 42:1186–1193, 2007.

[16] L. Brillouin. *Wave Propagation in Periodic Structures*. Dover, New York, NY, 1953.

[17] R. D. Cook, D. S. Malkus, M. E. Plesha, and R. J. Witt. *Concepts and Applications of Finite Element Analysis*. Wiley, 4^{th} edition, 2001.

[18] J. F. Doyle. *Wave Propagation in Structures*. Springer Verlag, second edition, 1997.

[19] K. L. Johnson. *Contact mechanics*. Cambridge University Press, Cambridge, UK, 2003.